Ceramics International 51 (2025) 5747–5753

Contents lists available at ScienceDirect

Ceramics International

journal homepage: www.elsevier.com/locate/ceramint

Pressureless joining of soda lime silicate glass using polysilazane-derived silica at near-room temperature

Levent Karacasulu [a,b,*], Mattia Biesuz [b,**], Virginia Pastorelli [c], Cekdar Vakifahmetoglu [a], Vincenzo M. Sglavo [b], Monica Ferraris [c], Gian D. Sorarù [b]

[a] Department of Materials Science and Engineering, İzmir Institute of Technology, İzmir, Türkiye
[b] Department of Industrial Engineering, University of Trento, Trento, Italy
[c] Department of Applied Science and Technology, Politecnico di Torino, Torino, Italy

ARTICLE INFO

Handling Editor: Dr P. Vincenzini

Keywords:
Glass
Joining
Pressureless joining
Perhydropolysilazane
Tensile strength

ABSTRACT

Perhydropolysilazane (PHPS) pre-ceramic polymer was used to join soda lime silicate glass at temperatures below 200 °C under pressureless conditions. The results show that: (i) the junction material is largely converted to silica at 100 °C and fully converted to glass at 150 °C; (ii) the samples treated at room temperature and 100 °C show a perfectly dense and clean bond, whereas porosity develops starting from 150 °C as a result of the hydrolysis reactions and solvent evaporation; (iii) a maximum tensile bond strength of about 5–6 MPa is obtained after treatments at 100 °C. Remarkably, after treatment at 500 °C, the junction remains intact. These preliminary findings provide the first successful attempt regarding the use of PHPS as a joining material to produce inorganic and transparent bonds for glass at relatively low temperatures.

1. Introduction

Differently from other materials like metals and polymers, joining of glass and ceramics still represents an almost unresolved challenge. Various technologies have been proposed in the past including diffusion bonding [1], nanocrystalline interlayer joining [2,3], transient eutectic-phase joining [4], MAX-phase joining [5], transient liquid-phase joining [6,7], laser joining [8] and flash joining [9,10] but the adhesion is often weak and the resistance limited in terms of service temperature range.

Pre-ceramic polymers have been sometimes employed to produce junctions between two ceramic components: a pre-ceramic resin used as joint material is cross-linked and pyrolyzed in inert atmosphere to allows its transformation to an inorganic compound (SiOC, SiO_2, SiC, Si_3N_4 etc.) [9,11–13]. Various pre-ceramic polymers such as polysilsesquioxane [12,14], polycarbosilane (PCS) [14–16], polysilazane [17] (PSZ), polycarbosilane (PCS)/polysilazane (PSZ) preceramic mixtures [18], polymethylsilane (PMS) [19] have been proposed in the past.

When glass components have to be joined, a quite obvious requirement is to preserve the transparency of the material, thus limiting the palette of possible bonding process. The most common techniques include adhesive bonding [20,21], glass soldering [22], diffusion bonding [23], laser beam welding [24–27], ultrasonic welding [28], thermal bonding [29], anodic bonding [30] and microelectroforming [31]. Among these, adhesive joining of glass components with organic compounds is quite frequent, it being simple and inexpensive. The three main types of adhesives that are used in such case are (i) UV-curable ones, (ii) epoxy-based ones and (iii) cyanoacrylates resins. Among them, the most common are UV-curable materials due to their low viscosity, despite the need of UV light equipment. Epoxy-based adhesives have the disadvantage of the high viscosity, while the curing time for cyanoacrylates is usually very short, thus limiting their diffuse applicability [31].

Perhydropolysilazane (PHPS) is a pre-ceramic polymer containing silicon, nitrogen and hydrogen, only. It is commercially available as a 20 wt% solution in di-n-butyl ether (DBE) because of its high reactivity with moisture [32]. Since it can react with oxygen and/or hydroxyl groups, it can easily transform into silica at low temperature in air [33]. For this reason, it is commonly used in the electronic industry to process spin-on silica coatings at room temperature on different substrates [34,35]. In addition, PHPS can be converted to amorphous ceramics under different controlled atmospheres such as ammonia [36–39], nitrogen

* Corresponding author. Department of Materials Science and Engineering, İzmir Institute of Technology, İzmir, Türkiye.
** Corresponding author.
E-mail addresses: levent.karacasulu@unitn.it, leventkaracasulu@gmail.com (L. Karacasulu), mattia.biesuz@unitn.it (M. Biesuz).

https://doi.org/10.1016/j.ceramint.2024.12.020
Received 7 May 2024; Received in revised form 1 December 2024; Accepted 2 December 2024
Available online 2 December 2024

[37,40], hydrogen peroxide [41], even under vacuum ultraviolet (VUV) light sources [33,42,43]. Consequently, for example, it forms SiO_x in the presence of oxygen or Si_3N_4 in the presence of nitrogen [44]. Due to its ability to self-crosslink in air or nitrogen even at low temperatures, combined with high chemical and thermal stability and excellent adhesion to various substrates, PHPS is highly suitable for coating applications [32]. This behavior can be attributed to the reactions with OH groups already present on the surface of several materials, this becoming fundamental in the formation of strong chemical bonding between coating and substrate [32,45]. Therefore, nowadays, PHPS is widely studied to obtain SiO_2 or Si_3N_4 coating [46] on different substrates such as aluminum [32], glass [36,47,48], fused silica [48], polycarbonate [49], polyethylene terephthalate [33,36,50], silicon [36] and steel [48,51,52] by using processes from room temperature to 1000 °C in air or nitrogen atmosphere. In addition, transparent coating on glass and PET by utilizing PHPS can be found in the literature [33,36,42,44,47,49,50].

Although PHPS is also a promising adhesive material for coating applications of glasses and ceramics (especially if one considers its possible conversion to an inorganic compound), a limited number of joining studies can be found in this field [53]. While it is known that PDCs can be used for joining applications, they are typically pyrolyzed at high temperatures (usually >800 °C) [13]. PHPS offers, therefore, some advantages including the possibility to cross-link and ceramize at near room temperature. Besides the energy consumption reduction, this allows an inorganic adhesive to join materials that cannot sustain the typical pyrolysis temperatures of PDCs, being well known that, for example, soda lime silicate glass certainly softens above 600 °C. Furthermore, PHPS leads to silica, which is transparent, while inorganic adhesives through the PDC route are typically black and opaque. Finally, the spontaneous hydration layer present on the glass surface is expected to facilitate the joint with PHPS. On these bases, the aim of the present work was to provide the first proof-of-concept of pressureless bonding of soda lime silicate glass at a temperature below 200 °C using PHPS.

2. Experimental procedure

Commercially available 4 mm thick soda lime silicate float glass (with nominal composition by weight: SiO_2 71.4 %, Al_2O_3 1.0 %, Na_2O 13.9 %, K_2O 0.3 %, MgO 4.1 %, CaO 9.1 %, other 0.2 %) was used in the present work. The original plate was cut using a diamond saw into small squares with nominal size 15 x 15 mm^2. The glasses were then cleaned by sonication in ethanol for 1 min and dried in air. Tin and air sides of the glass were identified using the typical “milky” fluorescence of tin under UVC light irradiation.

Perhydropolysilazane (PHPS) was purchased as a 20 wt% solution in dibutyl ether (DBE) from DurXtreme (tutoProm®, NN 120–20(A), DurXtreme GmbH, Uhlm, Germany). It was concentrated to ~50 wt% solution by evaporating DBE solvent at room temperature under vacuum. 12 µl of the concentrated PHPS solution was dropped in the middle of the “air side” glass surface with a micropipette. PHPS was allowed to spread onto the surface and then a second glass piece was gently leaned on the PHPS layer taking care to avoid the formation of air bubbles (Fig. 2). The PHPS solution was concentrated before the application to reduce the amount of solvent in the joint region and improve the joint quality. On the other hand, solutions concentrated above 50 wt% were quite viscous and difficult to be manipulated in air without oxidation. The prepared glass-PHP-glass joints were aged at room temperature (RT), 100 °C, 150 °C and 200 °C for 30 days.

The thermal behavior of PHPS was studied using thermogravimetric/thermodifferential analysis (TGA/DTA) using a Netzsch STA 409 thermobalance. The test was carried out in pure air flow up to 1000 °C with a heating rate of 5 °C/min. TGA/DTA were also repeated on PHPS aged for 30 days at 150 °C.

The morphology of the produced joints was investigated by scanning electron microscopy (SEM, JEOL JSM-5500, Japan). To observe the cross-section of the joints, the samples were polished in dry conditions to avoid any reaction between the polymer and water. Phase analysis was carried out by X-ray diffraction (XRD, Italstructures IPD3000 diffractometer, Italy) with a copper anode X-ray source (Cu-K_α radiation) on the joint samples’ fracture surfaces as obtained after the mechanical tests. FT-IR analyses were performed on the same surfaces using Varian 4100 FT-IR Excalibur series apparatus (Variant Inc, CA, USA) in ATR mode in the 4000 to 550 cm^{-1} range with 4 cm^{-1} resolution and 32 scans. The optical transmittance spectra of the samples were measured by JASCO V-570 spectrophotometer (Jasco, Inc., Tokyo, Japan) in the range of 300–1000 nm with a bandwidth of 1 nm.

The tensile strength of the joints treated at different temperatures was measured by a modification of ASTM C633-0139 norm [54] by using a mechanical testing machine (MTS Criterion model 43) equipped with a 5 kN load cell. Before testing, the samples were glued onto steel cylinders using a structural adhesive (DP 490 from 3M), which was cured for 48 h, according to the datasheet. The tensile test data set (load/stress vs. elongation) were acquired from three samples tested using a crosshead speed of 0.5 mm/min. The joints were also subjected to durability tests to investigate their thermal resistance up to 500 °C with a heating rate of 1 °C/min in air.

3. Results and discussion

All samples cured at room temperature, 100 °C and 150 °C remained perfectly joined after 1 month aging, whereas most of the samples treated at 200 °C were found separated or weakly bonded.

Fig. 1 shows the optical transmittance spectra of the joined materials treated at different temperature; the spectrum for the bare glass is also shown for comparison. The 4 mm thick glass has a transmittance just below 90 % in the visible range, similar to what is reported in the literature [55]. The transmittance of the ~8 mm thick joint samples slightly decreases with increasing the curing temperature. Whereas the sample treated at room temperature is characterized by a transmittance similar to bare monolithic glass, the specimens treated at higher temperature show oscillations in the spectra similarly to thin film-like behavior, probably due to possible interference effects in the joint region [56]. It is important to observe that although the transmittance of the joints is clearly lower compared to the single sheet, the ~8 mm thick joints (see inset in Fig. 1) are still highly very transparent in the visible range.

Fig. 2 shows the SEM micrographs of the polished joints after curing at different temperatures. The samples treated at room temperature,

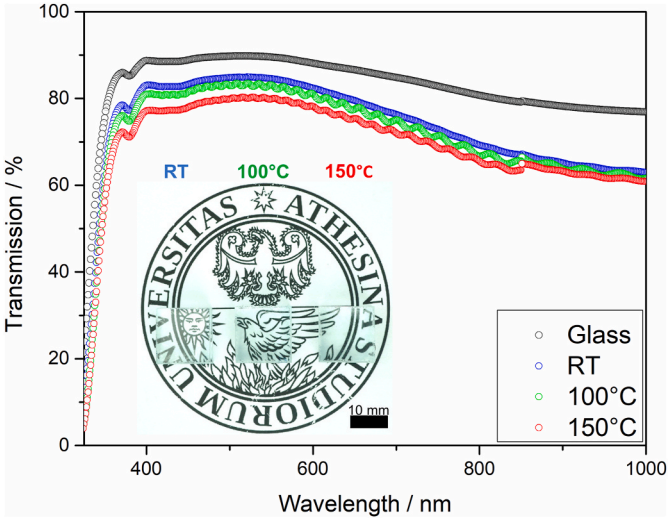

Fig. 1. Transmittance spectra of the 8 mm thick joints treated at room temperature, 100 °C and 150 °C; the spectrum recorded on 4 mm thick bare glass is also shown for comparison. The bonded samples are shown in the inset.

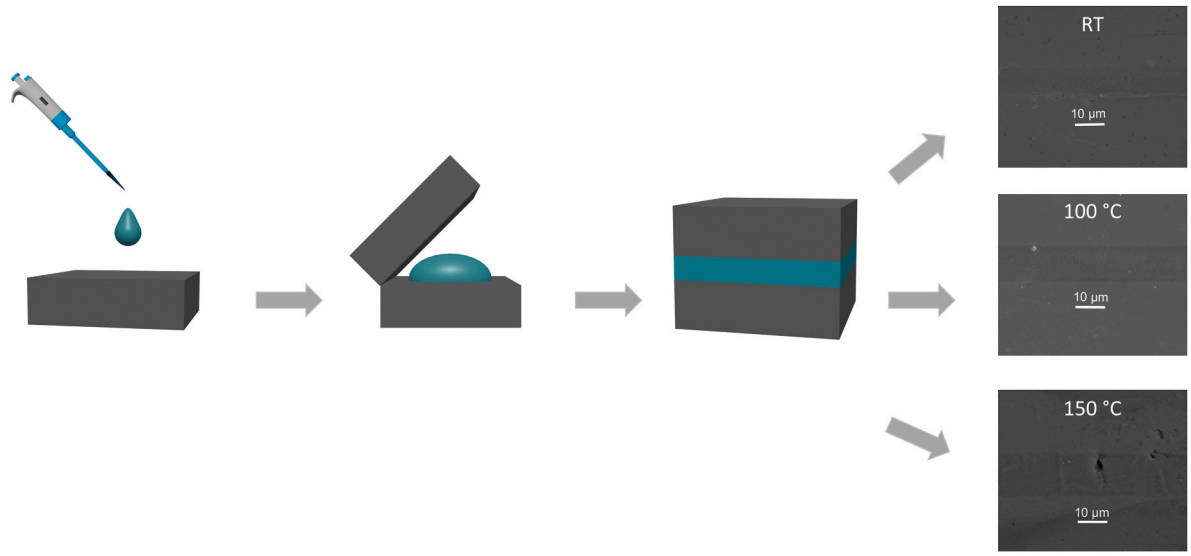

Fig. 2. Schematic illustration of the joint together with SEM micrographs of the polished cross-section of the samples after joining.

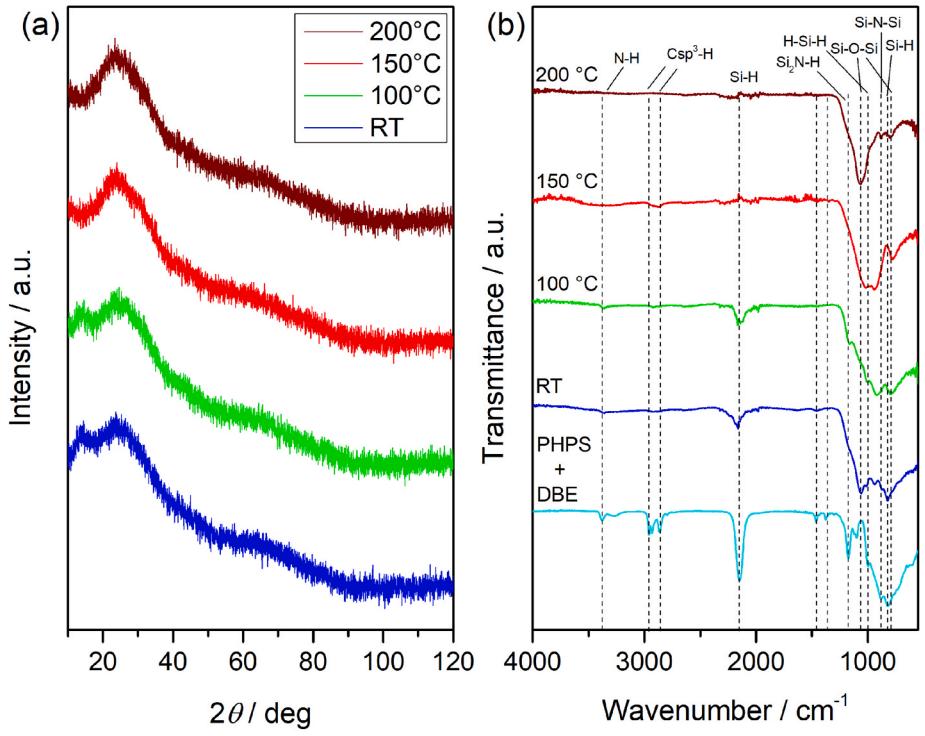

Fig. 3. **(a)** XRD patterns and **(b)** FTIR spectra of the joints obtained at different heat treatment temperatures.

100 °C and 150 °C show a clean and smooth interface between PHPS and glass. The joint thickness is in the micrometric range (about 10 µm) although it slightly increases with the treating temperatures. It should be noted that under said processing conditions, the thickness control may be challenging due to the manual joining procedure. In parallel with the joint swelling at 150 °C, one can observe the formation of pores which could originate from the gasses released upon cross-linking, solvent evaporation (which can also participate to the swelling) and densification. One could recall that the boiling temperature for DBE is 141 °C and this can lead to the formation of porosity during the treatment at 150 °C and to the joint failure at 200 °C [57].

XRD patterns were recorded on the joints after the mechanical tests (Fig. 3(a)). As expected, the samples heat-treated at different temperature are amorphous with no sign of crystallization. The pattern of the samples treated at RT and 100 °C is characterized by two amorphous humps, located at about 17–18° and 22°. The former can be attributed to a specific feature of the joining material, while the latter may correspond to either cross-linked feature of PHPS or silica glass-like structure [58] depending on x-ray penetration depth, this suggesting that PHPS was not completely converted into silica. On the other hand, the patterns

obtained on the samples aged at 150 °C and 200 °C, show only the feature at 22°, this pointing out a substantial conversion of the polymer into an inorganic silica glass by hydrolysis and polycondensation reactions.

Fig. 3(b) shows the FT-IR spectra of the samples prepared at RT, 100 °C, 150 °C and 200 °C together with starting pre-ceramic polymer. PHPS contains two main moieties (N-H and Si-H) possessing several absorption peaks at around 829 (Si-H wagging), 922 (Si-N-Si stretching), 955 (H-Si-H deformation), 1180 (Si_2N-H rocking), 2160 (Si-H stretching), and 3380 cm^{-1} (N-H stretching) [33,36,44,59,60]. In addition, DBE fingerprints are found as sp^3 C-H stretching at around 2960 and 2870 cm^{-1}, CH_2 bending at 1470 cm^{-1}, CH_3 bending at 1380 cm^{-1} and C-O stretching at 1180 cm^{-1} [61]. When the curing temperature is higher, the intensity of the Si-O-Si band, located at around 1060 cm^{-1} and 790 cm^{-1}, slowly increases [44,58,62–64], whereas the N-H and Si-H bands significantly (and even completely) disappear. The main peaks related to N-H and Si-N bonds are strongly reduced already at 100 °C while the Si-H moieties disappear at 150 °C suggesting that they are more resistant to hydrolysis than the N-H groups. The structural evolution observed by FTIR is fully consistent with the hydrolysis and condensation reaction of the Si-N and Si-H bonds of PHPS (Fig. 4) [50,53,65]. It is worth pointing out that FTIR analysis results suggest that the samples treated at 150 °C and 200 °C were largely converted into silica due to the negligible presence of Si-H and N-H vibrational features. This result perfectly agrees with the XRD patterns that indicates the presence of inorganic silica glass at such aging conditions within the detection limits.

The surface of the glass is usually hydrophilic because of the −OH groups. Accordingly, the adhesion of the coating on the glass is very likely due to the reaction of Si−OH groups with −NH− groups in PHPS. Due to its polarity, the Si—N bond is hydrophilic and can react with water, whereas the Si—H bond is typically hydrophobic. The Si—N content rapidly decreases and Si—O bonds are formed due to the rapid reaction of Si—NH—Si with Si-OH hydroxyl, while the reaction of Si—H groups with oxygen is slow and requires higher temperature. Therefore, a high concentration of Si—H bonds are maintained during the low-temperature annealing process (RT and 100 °C) [50]. Similarly, the sharp FTIR peak located at around 1180 cm^{-1} (Fig. 3) and assigned to the Si-NH-Si bond already diminished even in the samples treated at room temperature. The coating properties of PHPS, demonstrated in previous works due to its chemistry [32,46], led to distinguished results in the joining applications.

Fig. 5 shows the DTA/TGA analysis of the concentrated PHPS solution. Weight loss of around 39 % occurs up to around 225 °C. Above this temperature, ~5 % weight gain is recorded due to the polymer oxidation. The mass increase is coupled with an exothermic reaction at about 240 °C, which is related to the oxidation of PHPS into silica. Above 250 °C, no significant weight change can be observed. In addition, the residual weight of about 65 % after pyrolysis is consistent with the complete oxidation of a 50 wt% PHPS solution, thus confirming that the commercial solution was properly concentrated before being used for the joining. The formation of silica in the joints was observed at a slightly lower temperature (150–200 °C) than in TGA (250 °C). It is worth noting that TGA is carried out at a constant heating rate up to high temperature with no isotherms and it occurs in about 1 h, whereas the joints were aged for 30 days (i.e., for ≈720 h), thus anticipating the ceramization reactions. In order to confirm this, a PHPS sample was aged within a TGA crucible for 30 days at 100 °C and 150 °C. The

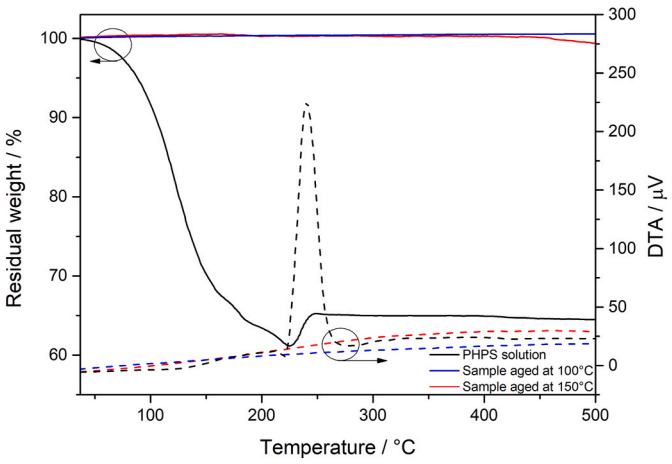

Fig. 5. DTA/TGA (dashed/continuous line) plots showing the temperature-dependent residual mass of the concentrated PHPS solution, and the sample aged at 100 °C and 150 °C (30 days).

material was afterward subjected to TGA/DTA analysis (Fig. 5). TGA plot shows substantially flat profiles, indicating a substantial ceramization of the sample during aging. More importantly, the DTA peak due to the polymer oxidation completely disappears in the aged compound. This confirms that the aging procedures used for the joint production at T > 100 °C cause a substantial conversion of the polymer into an inorganic compound.

Fig. 6 shows the effect of the heat treatment temperature on the tensile strength of the glass joints. A maximum is recorded for the samples treated at 100 °C (5–6 MPa), whereas the samples treated at 150 °C and room temperature exhibit modest resistance (about 1 MPa). The strength decreases from 100 °C to 150 °C can be attributed to the formation of pores within the joint, as shown in Fig. 2, due to the elimination of gaseous products and densification, validating the use of curing temperature below the DBE boiling point as in the previous study [53]. In any case, considering the mechanical test method (tensile), the results at 100 °C appear rather promising and interesting if compared with commercial UV-curable acrylates which reach about 5–20 MPa resistance with an adhesive layer thickness of about 1 mm [66].

In particular, it is worth noting that joining was carried out here without the application of any pressure, differently with respect to previous works [53]; it is thought that the application of pressure can increase the resistance of the joint by facilitating the formation of a clean interface, reducing the bond thickness and avoiding the formation of porosity. In addition, it is worth pointing out that future investigations could include more sophisticated approaches for the deposition of the PHPS (dip coating, spin coating and spray coating) [46].

Fig. 7 reports the fracture surface of the samples. For all samples, the fracture occurs within the joint in a cohesive mode. At room temperature and 100 °C the fracture is not smooth and microdomains and delaminated regions can be noted. The joints cured at 150 °C exhibit instead a relatively smooth fracture surface with features similar to inorganic glasses coherently with the FT-IR results.

The joints were finally subjected to durability tests to investigate their resistance up to 500 °C in air (i.e., about 60 °C below the glass transition temperature for the used soda lime silicate glass). All samples

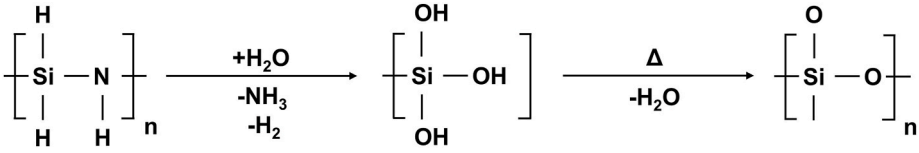

Fig. 4. Hydrolysis and polycondensation reactions for converting PHPS into silica at low temperatures and in the presence of moisture.

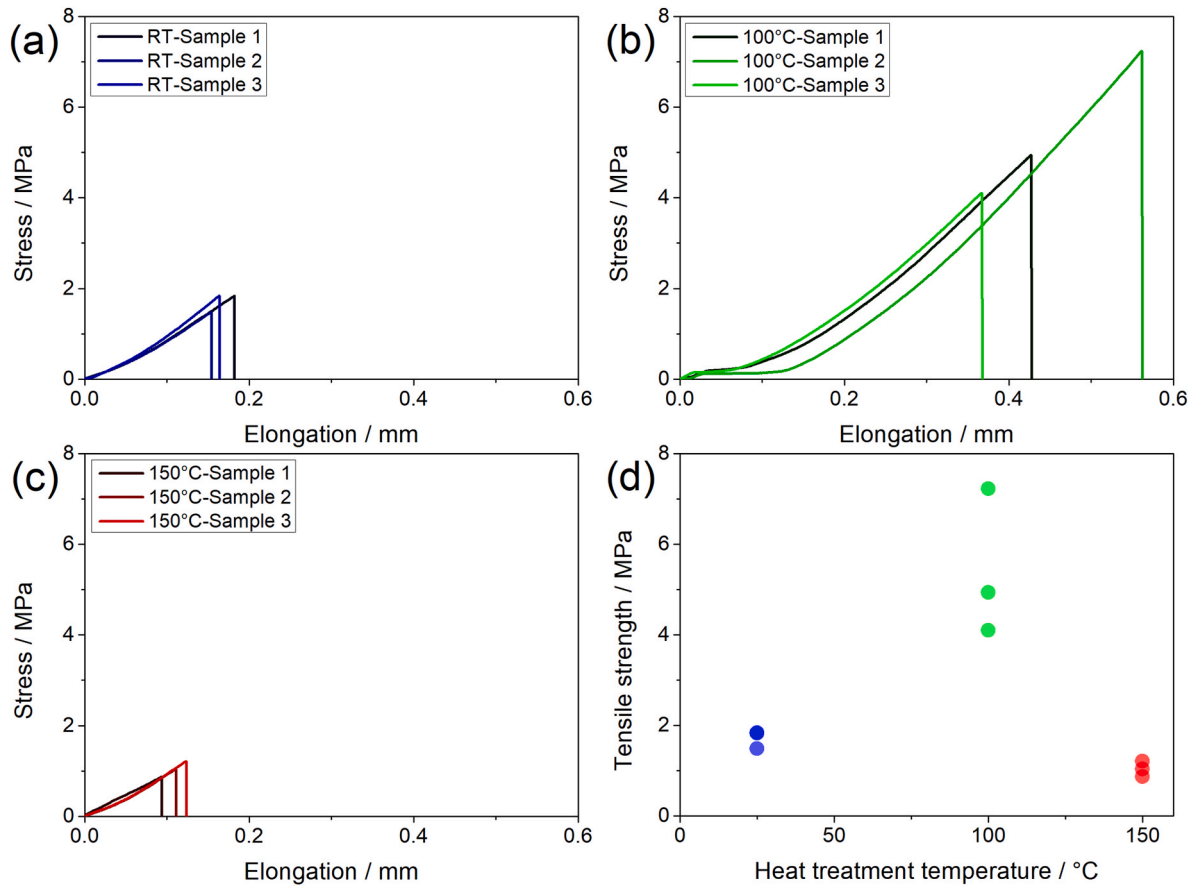

Fig. 6. Stress-elongation curves of the joints produced at **(a)** RT, **(b)** 100 °C, **(c)** 150 °C; **(d)** tensile strength values of the joints processed at different temperatures.

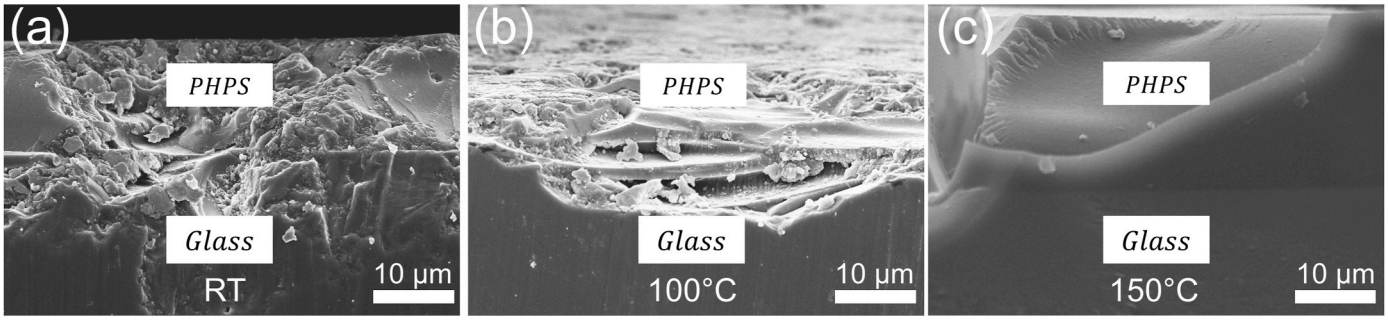

Fig. 7. SEM micrographs of the fracture surface cross-section of joints after tensile tests; joints cured at **(a)** RT, **(b)** 100 °C, and **(c)** 150 °C, respectively.

remained joined after such thermal treatment despite the transparency decreased, as expected. As such, PHPS can be considered as a joining material bond also other classes of inorganic materials operating at relatively high temperatures.

4. Conclusions

A novel adhesive bonding based on PHPS pre-ceramic polymer was investigated to join soda lime silicate glass below 200 °C in air. The optical transmittance of all joint samples slightly decreases with curing temperature. The samples aged at room temperature and 100 °C exhibit good adhesive properties, whereas pores are formed in the joint at 150 °C. The highest tensile strength, approximately 5–6 MPa, was achieved at a curing temperature of 100 °C, this validating the use of processing temperature below the DBE boiling point. Besides coating applications, PHPS can be considered as a potential candidate for the production of SiO_2-based joints stable at high temperatures.

CRediT authorship contribution statement

Levent Karacasulu: Writing – original draft, Visualization, Methodology, Investigation, Conceptualization. **Mattia Biesuz:** Writing – original draft, Methodology, Investigation, Data curation, Conceptualization. **Virginia Pastorelli:** Methodology, Investigation, Data curation. **Cekdar Vakifahmetoglu:** Writing – review & editing, Supervision. **Vincenzo M. Sglavo:** Writing – review & editing, Supervision, Resources. **Monica Ferraris:** Writing – review & editing, Supervision, Resources. **Gian D. Sorarù:** Writing – review & editing, Supervision, Resources.

Declaration of competing interest

The authors declare that they have no known competing financial interests or personal relationships that could have appeared to influence the work reported in this paper.

Acknowledgments

This work was supported by the European Office of Aerospace Research and Development, US Air Force Office of Scientific Research) within the project “From polymers to covalent glasses (PolGla)” Award Nr. FA8655-23-1-724.

References

[1] S. Rizzo, S. Grasso, M. Salvo, V. Casalegno, M.J. Reece, M. Ferraris, Joining of C/SiC composites by spark plasma sintering technique, J. Eur. Ceram. Soc. 34 (2014) 903–913, https://doi.org/10.1016/j.jeurceramsoc.2013.10.028.
[2] B.G. Ravi, R. Chaim, Joining of ZrO_2-4.5 wt% Y_2O_3 (Y-TZP) ceramics using nanocrystalline tape cast interlayers, J. Mater. Sci. 37 (2002) 813–818, https://doi.org/10.1023/A:1013804301381.
[3] R. Chaim, B.G. Ravi, Joining of alumina ceramics using nanocrystalline tape cast interlayer, J. Mater. Res. 15 (2000) 1724–1728, https://doi.org/10.1557/JMR.2000.0248.
[4] Y. Katoh, L.L. Snead, T. Cheng, C. Shih, W.D. Lewis, T. Koyanagi, T. Hinoki, C. H. Henager, M. Ferraris, Radiation-tolerant joining technologies for silicon carbide ceramics and composites, J. Nucl. Mater. 448 (2014) 497–511, https://doi.org/10.1016/j.jnucmat.2013.10.002.
[5] P. Tatarko, V. Casalegno, C. Hu, M. Salvo, M. Ferraris, M.J. Reece, Joining of CVD-SiC coated and uncoated fibre reinforced ceramic matrix composites with pre-sintered Ti_3SiC_2 MAX phase using Spark Plasma Sintering, J. Eur. Ceram. Soc. 36 (2016) 3957–3967, https://doi.org/10.1016/j.jeurceramsoc.2016.06.025.
[6] M. Ferraris, M. Salvo, C. Isola, M. Appendino Montorsi, A. Kohyama, Glass-ceramic joining and coating of SiC/SiC for fusion applications, J. Nucl. Mater. 258–263 (1998) 1546–1550, https://doi.org/10.1016/S0022-3115(98)00176-7.
[7] S.J. Glass, F.M. Mahoney, B. Quillan, J.P. Pollinger, R.E. Loehman, Refractory oxynitride joints in silicon nitride, Acta Mater. 46 (1998) 2393–2399, https://doi.org/10.1016/S1359-6454(98)80021-9.
[8] W. Lippmann, J. Knorr, R. Wolf, R. Rasper, H. Exner, A.-M. Reinecke, M. Nieher, R. Schreiber, Laser joining of silicon carbide—a new technology for ultra-high temperature resistant joints, Nucl. Eng. Des. 231 (2004) 151–161, https://doi.org/10.1016/j.nucengdes.2004.03.002.
[9] M. Biesuz, T.G. Saunders, S. Grasso, G. Speranza, G.D. Sorarù, R. Campostrini, V. M. Sglavo, M.J. Reece, Flash joining of conductive ceramics in a few seconds by flash spark plasma sintering, J. Eur. Ceram. Soc. 39 (2019) 4664–4672, https://doi.org/10.1016/j.jeurceramsoc.2019.07.036.
[10] J. Xia, W. Ren, Y. Zhang, T. Xu, C. Li, X. Shao, K. Ren, Y. Wang, Fast joining of 8YSZ to NiCrFe medium-entropy alloy by using an electric field, J. Eur. Ceram. Soc. 43 (2023) 4431–4436, https://doi.org/10.1016/j.jeurceramsoc.2023.03.047.
[11] P. Colombo, G. Mera, R. Riedel, G.D. Sorarù, Polymer-Derived ceramics: 40 Years of Research and innovation in advanced ceramics, J. Am. Ceram. Soc. 93 (2010) 1805–1837, https://doi.org/10.1111/j.1551-2916.2010.03876.x.
[12] P. Colombo, V. Sglavo, E. Pippel, J. Woltersdorf, Joining of reaction-bonded silicon carbide using a preceramic polymer, J. Mater. Sci. 33 (1998) 2405–2412, https://doi.org/10.1023/A:1004312109836.
[13] C.A. Lewinsohn, P. Colombo, I. Reimanis, Ö. Ünal, Stresses occurring during joining of ceramics using preceramic polymers, J. Am. Ceram. Soc. 84 (2001) 2240–2244, https://doi.org/10.1111/j.1151-2916.2001.tb00995.x.
[14] P. Colombo, A. Donato, B. Riccardi, J. Woltersdorf, E. Pippel, R. Silberglitt, G. Danko, Joining SiC-based ceramics and composites with preceramic polymers, in: Advanced SiC/SiC Ceramic Composites: Developments and Applications in Energy Systems, 2006, pp. 323–334, https://doi.org/10.1002/9781118406014.ch29.
[15] C.-C. Zhao, R.-L. Lin, M.-M. Dai, X. Xu, L.-L. Zhu, J.-X. Xue, J.-H. Zhai, H.-B. Ma, W.-M. Guo, H.-T. Lin, Q.-S. Ren, Y.-H. Liao, Facile joining of SiC ceramics with screen-printed polycarbosilane without pressure, J. Eur. Ceram. Soc. 41 (2021) 2157–2161, https://doi.org/10.1016/j.jeurceramsoc.2020.10.042.
[16] Y. Chen, Y. Cao, Y. Wang, Electrical property of joints made of polymer-derived SiAlCN ceramic via adhesive joining, Ceram. Int. 47 (2021) 3649–3656, https://doi.org/10.1016/j.ceramint.2020.09.216.
[17] J. Xue, Y. Hou, W. Chu, Y. Yang, L. Zhang, G. Wen, Advanced pressurelessly prepared adhesive composites based on modified preceramic polymer for the joining of amorphous SiBON ceramics, Ceram. Int. 49 (2023) 26847–26859, https://doi.org/10.1016/j.ceramint.2023.05.221.
[18] D.-H. Jeong, A. Septiadi, P. Fitriani, D.-H. Yoon, Joining of SiC_f/SiC using polycarbosilane and polysilazane preceramic mixtures, Ceram. Int. 44 (2018) 10443–10450, https://doi.org/10.1016/j.ceramint.2018.03.061.
[19] X. Wang, J. Wang, H. Wang, Joining of SiC ceramics via a novel liquid preceramic polymer (V-PMS), Ceram. Int. 41 (2015) 7283–7288, https://doi.org/10.1016/j.ceramint.2015.02.008.
[20] F. Oikonomopoulou, F. Veer, R. Nijsse, K. Baardolf, A completely transparent, adhesively bonded soda-lime glass block masonry system, J. Facade Des. Eng. 2 (2014) 201–221, https://doi.org/10.3233/FDE-150021.
[21] Y.-J. Pan, R.-J. Yang, A glass microfluidic chip adhesive bonding method at room temperature, J. Micromech. Microeng. 16 (2006) 2666, https://doi.org/10.1088/0960-1317/16/12/020.
[22] R.G. Frieser, A review of solder glasses, Electrocompon. Sci. Technol. 2 (1975) 509270, https://doi.org/10.1155/APEC.2.163.
[23] I. Drozdowska-Rusinowicz, Diffusion bonding of glass to metals with reference to quartz-aluminium bonding, Weld. Int. 1 (1987) 544–547, https://doi.org/10.1080/09507118709449362.
[24] T. Tamaki, W. Watanabe, J. Nishii, K. Itoh, Welding of transparent materials using femtosecond laser pulses, Jpn. J. Appl. Phys. 44 (2005) L687, https://doi.org/10.1143/JJAP.44.L687.
[25] W. Watanabe, S. Onda, T. Tamaki, K. Itoh, Direct joining of glass substrates by 1 kHz femtosecond laser pulses, Appl. Phys. B 87 (2007) 85–89, https://doi.org/10.1007/s00340-006-2537-y.
[26] R. Cruz, J.A. da C. Ranita, J. Macaira, F. Ribeiro, A.M.B. da Silva, J.M. Oliveira, M. H.F. V Fernandes, H.A. Ribeiro, J.G. Mendes, A. Mendes, Glass–glass laser-assisted glass frit bonding, IEEE Trans. Compon. Packag. Manuf. Technol. 2 (2012) 1949–1956, https://doi.org/10.1109/TCPMT.2012.2212195.
[27] X. Jia, K. Li, Z. Li, C. Wang, J. Chen, S. Cui, Multi-scan picosecond laser welding of non-optical contact soda lime glass, Opt Laser. Technol. 161 (2023) 109164, https://doi.org/10.1016/j.optlastec.2023.109164.
[28] G. Wagner, F. Walther, T. Nebel, D. Eifler, Glass/glass joints by ultrasonic welding, Glass Technol. 44 (2003) 152–155.
[29] N.F. Raley, J.C. Davidson, J.W. Balch, Examination of glass-silicon and glass-glass bonding techniques for microfluidic systems, Proc. SPIE (1995) 40–45, https://doi.org/10.1117/12.221298.
[30] J. Wei, S.M.L. Nai, C.K. Wong, L.C. Lee, Glass-to-glass anodic bonding process and electrostatic force, Thin Solid Films 462–463 (2004) 487–491, https://doi.org/10.1016/j.tsf.2004.05.067.
[31] Joining methods for glass based microdevices, in: D. Hülsenberg, A. Harnisch, A. Bismarck (Eds.), Microstructuring of Glasses, Springer Berlin Heidelberg, Berlin, Heidelberg, 2008, pp. 263–278, https://doi.org/10.1007/978-3-540-49888-9_10.
[32] G. Barroso, M. Döring, A. Horcher, A. Kienzle, G. Motz, Polysilazane-based coatings with anti-adherent properties for easy release of plastics and composites from metal molds, Adv. Mater. Interfac. 7 (2020) 1901952, https://doi.org/10.1002/admi.201901952.
[33] Y. Naganuma, T. Horiuchi, C. Kato, S. Tanaka, Low-temperature synthesis of silica coating on a poly(ethylene terephthalate) film from perhydropolysilazane using vacuum ultraviolet light irradiation, Surf. Coat. Technol. 225 (2013) 40–46, https://doi.org/10.1016/j.surfcoat.2013.03.014.
[34] S.-D. Kim, P.-S. Ko, K.-S. Park, Perhydropolysilazane spin-on dielectrics for inter-layer-dielectric applications of sub-30 nm silicon technology, Semicond. Sci. Technol. 28 (2013) 035008, https://doi.org/10.1088/0268-1242/28/3/035008.
[35] S.M. Kim, H.C. Kim, J. Bang, D. Yoon, E. Koo, Fabrication and characterization of the barrier film having excellent moisture barrier characteristics using polysilazane, J. Nanosci. Nanotechnol. 20 (2020) 5662–5666, https://doi.org/10.1166/jnn.2020.17618.
[36] H. Kozuka, M. Fujita, S. Tamoto, Polysilazane as the source of silica: the formation of dense silica coatings at room temperature and the new route to organic–inorganic hybrids, J. Sol. Gel Sci. Technol. 48 (2008) 148–155, https://doi.org/10.1007/s10971-008-1793-1.
[37] C.R. Blanchard, S.T. Schwab, X-Ray diffraction analysis of the pyrolytic conversion of perhydropolysilazane into silicon nitride, J. Am. Ceram. Soc. 77 (1994) 1729–1739, https://doi.org/10.1111/j.1151-2916.1994.tb07043.x.
[38] T. Kubo, E. Tadaoka, H. Kozuka, Formation of silica coating films from spin-on polysilazane at room temperature and their stability in hot water, J. Mater. Res. 19 (2004) 635–642, https://doi.org/10.1557/jmr.2004.19.2.635.
[39] T. Kubo, E. Tadaoka, H. Kozuka, Preparation of hot water-resistant silica thin films from polysilazane solution at room temperature, J. Sol. Gel Sci. Technol. 31 (2004) 257–261, https://doi.org/10.1023/B:JSST.0000047999.87439.c2.
[40] M. Biesuz, P. Bettotti, S. Signorini, M. Bortolotti, R. Campostrini, M. Bahri, O. Ersen, G. Speranza, A. Lale, S. Bernard, G.D. Sorarù, First synthesis of silicon nanocrystals in amorphous silicon nitride from a preceramic polymer, Nanotechnology 30 (2019) 255601, https://doi.org/10.1088/1361-6528/ab0cc8.
[41] J.-S. Lee, J.-H. Oh, S.-W. Moon, W.-S. Sul, S.-D. Kim, A technique for converting perhydropolysilazane to SiO_x at low temperature, Electrochem. Solid State Lett. 13 (2010) H23, https://doi.org/10.1149/1.3264092.
[42] L. Prager, A. Dierdorf, H. Liebe, S. Naumov, S. Stojanović, R. Heller, L. Wennrich, M.R. Buchmeiser, Conversion of perhydropolysilazane into a SiO_x network triggered by vacuum ultraviolet irradiation: access to flexible, transparent barrier coatings, Chem. Eur J. 13 (2007) 8522–8529, https://doi.org/10.1002/chem.200700351.
[43] N. Shinde, Y. Takano, J. Sagan, V. Monreal, T. Nagahara, Spin-on silicon-nitride films for photo-lithography by RT cure of polysilazane, J. Photopolym. Sci. Technol. 23 (2010) 225–230, https://doi.org/10.2494/photopolymer.23.225.
[44] K. Wang, M. Günthner, G. Motz, B.D. Flinn, R.K. Bordia, Control of surface energy of silicon oxynitride films, Langmuir 29 (2013) 2889–2896, https://doi.org/10.1021/la304307y.
[45] D. Amouzou, L. Fourdrinier, F. Maseri, R. Sporken, Formation of Me–O–Si covalent bonds at the interface between polysilazane and stainless steel, Appl. Surf. Sci. 320 (2014) 519–523, https://doi.org/10.1016/j.apsusc.2014.09.109.

[46] G. Barroso, Q. Li, R.K. Bordia, G. Motz, Polymeric and ceramic silicon-based coatings – a review, J Mater Chem A Mater 7 (2019) 1936–1963, https://doi.org/10.1039/C8TA09054H.
[47] M. Monti, B. Dal Bianco, R. Bertoncello, S. Voltolina, New protective coatings for ancient glass: silica thin-films from perhydropolysilazane, J. Cult. Herit. 9 (2008) e143–e145, https://doi.org/10.1016/j.culher.2008.08.002.
[48] M. Günthner, K. Wang, R.K. Bordia, G. Motz, Conversion behaviour and resulting mechanical properties of polysilazane-based coatings, J. Eur. Ceram. Soc. 32 (2012) 1883–1892, https://doi.org/10.1016/j.jeurceramsoc.2011.09.005.
[49] Y. Zhan, R. Grottenmüller, W. Li, F. Javaid, R. Riedel, Evaluation of mechanical properties and hydrophobicity of room-temperature, moisture-curable polysilazane coatings, J. Appl. Polym. Sci. 138 (2021) 50469, https://doi.org/10.1002/app.50469.
[50] Z. Zhang, Z. Shao, Y. Luo, P. An, M. Zhang, C. Xu, Hydrophobic, transparent and hard silicon oxynitride coating from perhydropolysilazane, Polym. Int. 64 (2015) 971–978, https://doi.org/10.1002/pi.4871.
[51] M. Günthner, T. Kraus, W. Krenkel, G. Motz, A. Dierdorf, D. Decker, Particle-filled PHPS silazane-based coatings on steel, Int. J. Appl. Ceram. Technol. 6 (2009) 373–380, https://doi.org/10.1111/j.1744-7402.2008.02346.x.
[52] M. Günthner, T. Kraus, A. Dierdorf, D. Decker, W. Krenkel, G. Motz, Advanced coatings on the basis of Si(C)N precursors for protection of steel against oxidation, J. Eur. Ceram. Soc. 29 (2009) 2061–2068, https://doi.org/10.1016/j.jeurceramsoc.2008.11.013.
[53] L. Duo, Z. Zhang, K. Zheng, D. Wang, C. Xu, Y. Xia, Perhydropolysilazane derived SiON interfacial layer for Cu/epoxy molding compound composite, Surf. Coat. Technol. 391 (2020) 125703, https://doi.org/10.1016/j.surfcoat.2020.125703.
[54] F. Smeacetto, M. Salvo, M. Ferraris, V. Casalegno, P. Asinari, A. Chrysanthou, Characterization and performance of glass–ceramic sealant to join metallic interconnects to YSZ and anode-supported-electrolyte in planar SOFCs, J. Eur. Ceram. Soc. 28 (2008) 2521–2527, https://doi.org/10.1016/j.jeurceramsoc.2008.03.035.
[55] D.A. Schaeffer, G. Polizos, D.B. Smith, D.F. Lee, S.R. Hunter, P.G. Datskos, Optically transparent and environmentally durable superhydrophobic coating based on functionalized SiO_2 nanoparticles, Nanotechnology 26 (2015) 055602, https://doi.org/10.1088/0957-4484/26/5/055602.
[56] N. Memarian, S.M. Rozati, I. Concina, A. Vomiero, Deposition of nanostructured CdS thin films by thermal evaporation method: effect of substrate temperature, Materials 10 (2017) 773, doi:10.3390/ma10070773.
[57] B. Spingler, S. Schnidrig, T. Todorova, F. Wild, Some thoughts about the single crystal growth of small molecules, CrystEngComm 14 (2012) 751–757, https://doi.org/10.1039/C1CE05624G.
[58] L. Karacasulu, E. Ogur, C. Piskin, C. Vakifahmetoglu, Cold sintering of soda-lime glass, Scripta Mater. 192 (2021) 111–114, https://doi.org/10.1016/j.scriptamat.2020.10.015.
[59] H.J. Seul, H.-G. Kim, M.-Y. Park, J.K. Jeong, A solution-processed silicon oxide gate dielectric prepared at a low temperature via ultraviolet irradiation for metal oxide transistors, J Mater Chem C Mater 4 (2016) 10486–10493, https://doi.org/10.1039/C6TC03725A.
[60] A. Zambotti, M. Biesuz, R. Campostrini, S.M. Carturan, G. Speranza, R. Ceccato, F. Parrino, G.D. Sorarù, Synthesis and thermal evolution of polysilazane-derived SiCN(O) aerogels with variable C content stable at 1600 °C, Ceram. Int. 47 (2021) 8035–8043, https://doi.org/10.1016/j.ceramint.2020.11.157.
[61] D.L. Pavia, G.M. Lampman, G.S. Kriz, J.A. Vyvyan, Introduction to Spectroscopy, Cengage learning, 2014.
[62] Y.-K. Lee, Y.L. Peng, M. Tomozawa, IR reflection spectroscopy of a soda-lime glass surface during ion-exchange, J. Non-Cryst. Solids 222 (1997) 125–130, https://doi.org/10.1016/S0022-3093(97)90104-6.
[63] J. Osswald, K.T. Fehr, FTIR spectroscopic study on liquid silica solutions and nanoscale particle size determination, J. Mater. Sci. 41 (2006) 1335–1339, https://doi.org/10.1007/s10853-006-7327-8.
[64] F. Bauer, U. Decker, A. Dierdorf, H. Ernst, R. Heller, H. Liebe, R. Mehnert, Preparation of moisture curable polysilazane coatings: Part I. Elucidation of low temperature curing kinetics by FT-IR spectroscopy, Prog. Org. Coating 53 (2005) 183–190, https://doi.org/10.1016/j.porgcoat.2005.02.006.
[65] S.Y. Je, B.-G. Son, H.-G. Kim, M.-Y. Park, L.-M. Do, R. Choi, J.K. Jeong, Solution-processable $LaZrO_x/SiO_2$ gate dielectric at low temperature of 180 °C for high-performance metal oxide field-effect transistors, ACS Appl. Mater. Interfaces 6 (2014) 18693–18703, https://doi.org/10.1021/am504231h.
[66] K. Machalická, M. Eliášová, Adhesive joints in glass structures: effects of various materials in the connection, thickness of the adhesive layer, and ageing, Int. J. Adhesion Adhes. 72 (2017) 10–22, https://doi.org/10.1016/j.ijadhadh.2016.09.007.